

Knudsen Cell Studies of the Reaction of Gaseous Nitric Acid with Synthetic Sea Salt at 298 K

D. O. De Haan[†] and B. J. Finlayson-Pitts*

Department of Chemistry, University of California, Irvine, Irvine, California 92697-2025

Received: July 28, 1997; In Final Form: September 30, 1997[⊗]

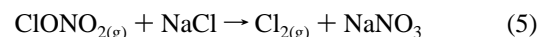
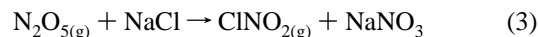
The uptake of nitric acid on synthetic sea salt (SSS) was studied at 298 K using a Knudsen cell with mass spectrometric detection of the gaseous reactant and products. HCl was the only product observed, with yields of 100% within experimental error. Nitric acid reaction probabilities decreased with reaction time by a factor of ~ 2 – 3 , ultimately reaching a constant value. Both the higher initial reaction probabilities (which ranged from 0.07 to 0.75) and the final steady-state values (which ranged from 0.03 to 0.25) decreased if the salt had been heated at 75 °C while pumping to decrease the amount of water on the salt surface prior to reaction. Several experiments using $\text{MgCl}_2 \cdot 6\text{H}_2\text{O}$ also gave very large nitric acid reaction probabilities, ≥ 0.14 in all cases, consistent with the important role of crystalline hydrates in the reactivity of SSS observed in earlier studies. The presence of large amounts of water on the SSS surface was illustrated by two phenomena: (1) the uptake of D_2O and liberation of large amounts of HDO and smaller amounts of H_2O and (2) the formation of gaseous HCl, rather than DCl, as the major product of the DNO_3 reaction with SSS. The results of these experiments confirm the critical role of surface-adsorbed water in the uptake and reaction of HNO_3 with salt surfaces, as proposed earlier based on similar studies of the reaction of HNO_3 with NaCl. They also suggest that the reaction probability for HNO_3 with sea salt particles below the deliquescence point is approximately an order of magnitude larger than for reaction with pure NaCl, the major component of these particles. The atmospheric implications are discussed.

Introduction

Over the past decade, atmospheric reactions involving particles, fogs, and clouds have been shown to be important. For example, in the stratosphere, surface chemistry occurring on polar stratospheric clouds, background sulfate aerosol, and perhaps cirrus clouds¹ has been shown to have major effects on ozone destruction rates via changes in the chemical partitioning of nitrogen oxides and chlorine compounds. In the troposphere, reactions of sea salt particles that generate gaseous photochemically active halogen compounds have been of great interest.^{2–8}

Sea salt spray is a major source of particles in the lower atmosphere, especially in the marine boundary layer and in coastal areas.⁹ Wind and wave action create a wide size distribution of seawater aerosol droplets, from which water evaporates at low humidities ($< 50\%$ relative humidity) to form solid particles.¹⁰ While it might be expected that sea salt particles have the same ionic composition as seawater, these particles are often found to be partially depleted of chloride and bromide ions under a variety of conditions.^{4,11–13} This loss of particle-phase chloride and bromide suggests the existence of a source of gas-phase, halogen-containing compounds in the marine boundary layer and in coastal areas.^{3,4,12}

The following reactions of NaCl, the major component of these particles, have been shown to occur:^{3–5,14–44}



The first two reactions produce gas-phase HCl, believed to be the most abundant form of chlorine in the marine environment. HCl is not photolyzed and is rapidly scavenged by fog and cloud particles. However, the reactions of N_2O_5 , NO_2 , ClONO_2 , and likely HOCl with NaCl produce compounds that are efficiently photolyzed to produce atomic chlorine.⁴⁵

Since atomic chlorine is more reactive toward organics than OH radicals,⁴⁵ the existence of an atomic chlorine source may prove significant for initiating atmospheric oxidation of organics,^{2,46,47} especially at sunrise. Although direct field measurements of atomic chlorine and its precursors (e.g., Cl_2 , ClNO_2 , HOCl) are extremely difficult, Cl_2 has recently been detected and measured in the marine boundary layer.⁴⁸ Additionally, indirect field detection of chlorine compounds other than HCl using mist chambers,⁴⁹ a photochemical technique,⁵⁰ and the analysis of hydrocarbon ratios to determine relative Cl and OH initiated oxidation rates^{51–53} have been used to estimate atomic chlorine concentrations. Estimates of peak sunrise chlorine concentrations in the marine boundary layer range from 10^3 to 10^5 cm^{-3} ,^{46,48–53} although the average global levels over the whole troposphere are smaller.^{54,55}

Most laboratory studies have used NaCl as a model for sea salt since it is the most abundant component (77% w/w).^{2,56} However, recent DRIFTS (diffuse reflectance infrared Fourier transform spectroscopy) measurements⁵⁷ suggest that NaCl may not be the component of sea salt which is most reactive with HNO_3 . This study of surface nitrate produced in reactions 1 and 4 indicates that HNO_3 and NO_2 appear to react preferentially with hydrate salts such as magnesium chloride hexahydrate

[†] Current address: Department of Chemistry and Biology, Lyon College, 2300 Highland Rd., P.O. Box 2317, Batesville, AR 72503-2317.

* To whom correspondence should be addressed. E-mail bjfinlay@uci.edu; phone (714) 824-7670; FAX (714) 824-3168.

[⊗] Abstract published in *Advance ACS Abstracts*, November 15, 1997.

($\text{MgCl}_2 \cdot 6\text{H}_2\text{O}$). In addition, studies of sea salt aerosol in the presence of ozone and NO_x have shown enhanced production of atomic chlorine relative to experiments using pure NaCl aerosol.^{29,33} These recent results imply that laboratory measurements of reactions 1–5 with NaCl may not be quantitatively extrapolated to reactions on sea salt aerosol in the troposphere.

Previous work⁵⁸ has provided strong evidence for the existence on NaCl powders of strongly adsorbed water (SAW) which cannot be evaporated by gentle heating under vacuum. In that work, HCl and DCl production were measured in two types of reactions of NaCl: (1) reaction with DNO_3 and (2) HNO_3 reaction with NaCl that had been previously exposed to gaseous D_2O .⁵⁸ These studies led to the hypothesis of SAW which controlled the uptake and subsequent reaction of HNO_3 . The initial uptake of HNO_3 for unheated salts was larger than the steady-state value, which was attributed to two types of surface sites holding water. The first type of water adsorption site could be destroyed by reaction with HNO_3 (such as water adsorbed on a surface OH^- site).^{59,60} The second type, responsible for the steady-state uptake, was attributed to water adsorption at other sites such as surface defects, steps, and edges. The reaction probabilities derived from the steady-state uptake of HNO_3 were the same for coarse and fine NaCl particle sizes, $\gamma = (1.4 \pm 0.6) \times 10^{-2}$. This was in excellent agreement with other studies using NaCl powders^{37,38,41} but greater than that for reaction with (100) single crystals [$\gamma = (4 \pm 2) \times 10^{-4}$], which do not hold SAW.⁶¹ Recently, Shindo et al.⁶² reported atomic force microscopy studies showing that natural rock salt crystals of NaCl had voids in the surface which were sites for the uptake of three-dimensional water. Such voids, if generally characteristic of NaCl surfaces, could be the sites for the SAW in our earlier studies.⁵⁸

The goal of the present experiment is to measure reaction probabilities for nitric acid with synthetic sea salt powders. The contribution of crystalline hydrates to total SSS reactivity is also directly probed by studying the uptake of HNO_3 on $\text{MgCl}_2 \cdot 6\text{H}_2\text{O}$, the most abundant crystalline hydrate.^{56,57} Additional evidence of the controlling influence of surface-bound water on nitric acid reactivity at salt surfaces is presented, confirming the model for uptake and reaction of HNO_3 on salt surfaces presented earlier.⁵⁸ Finally, we use these data to recommend atmospheric reaction probabilities for HNO_3 with sea salt particles.

Experimental Section

The experiments were performed using a Knudsen cell which has been described previously.⁵⁸ Cell walls and the salt sample holder were heatable to 75–80 °C (limited by the temperature at which the halocarbon wax starts to flow) by a fluid circulator (Lauda RC6). All exposed surfaces were coated with halocarbon wax (Halocarbon Products Corp.) to minimize uptake of gases on the reactor walls. Surface uptake measurements are based on the competition between loss of the reactant to the reactive surface and its loss through a variable-sized exit orifice into the differentially pumped mass spectrometer chamber. A movable lid over the salt sample holder allows it to be isolated from gases flowing through the cell by an O-ring seal, with minimal change in cell volume (<1%) as the lid is opened. By opening and closing the lid while monitoring reactant signal in the mass spectrometer, the two loss processes can be quantified relative to each other. The reaction probability is given by

$$\gamma = \frac{A_h N_0 - N_r}{A_s N_r} \quad (1)$$

where A_h is the area of the exit orifice, A_s is the area of the reactive surface, N_r is the reactant signal with the reactive surface exposed, and N_0 is the signal with the surface covered. All experiments were performed in continuous flow mode. As discussed below, HCl is the only product detected and is formed at 100% yield, within experimental error. Hence, our measurements based on net uptake of HNO_3 are, in effect, reaction probabilities, the term we shall use throughout this work.

Samples of sodium chloride were prepared by grinding pieces of single-crystal NaCl windows (Harshaw Bicon) in a stainless steel ball grinder (Wig-L-Bug) for 5 min. Synthetic sea salt (Instant Ocean, Aquarium Systems; see ref 57 for composition) and magnesium chloride hexahydrate (Sigma, ACS Grade) either were used as received as coarse particles or were ground into finer particles using the same procedure as for NaCl. Both salts were heated at 100 °C overnight and stored in a desiccator prior to grinding. This preliminary drying does not eliminate all of the adsorbed water since water is readily reabsorbed from room air during subsequent handling. Previously published analyses by scanning electron microscopy and volumetric BET surface area determinations of fine NaCl and synthetic sea salt powders⁵⁷ indicate that these grinding processes result in mean particle diameters of approximately 2.4 and 0.3 μm and total surface areas of 1.2×10^4 for NaCl and $9.4 \times 10^4 \text{ cm}^2 \text{ g}^{-1}$ for SSS, respectively. The ground salts are referred to as “fine” and the unground as “coarse” throughout.

Immediately after grinding, salt samples were packed into a shallow Teflon sample holder (diameter 30.8 or 49 mm), weighed, and placed in the Knudsen cell. The salt was pumped for a minimum of 2 h while the Knudsen cell walls were heated at 75–80 °C to remove adsorbed water. In some experiments the salt was heated simultaneously at the same temperature. The salt sample was then isolated from the Knudsen cell by covering it with the lid as the cell and sample were cooled back to room temperature before the start of the experiment.

Gaseous nitric acid was generated using a 2:1 (v/v) mixture of concentrated sulfuric acid (96%, Fisher Reagent ACS grade) and nitric acid (69%, Fisher ACS Plus grade). Liquid deionized water was the source of H_2O vapor. Both were subjected to at least three freeze–pump–thaw cycles to remove dissolved gases. Deuterated gas sources were made by the same procedures, but transfers to the bulbs were done in nitrogen-filled glovebags to avoid uptake of H_2O from ambient air. Deuterated water was supplied by Cambridge Isotope Laboratories (99.9% D). Deuterated nitric and sulfuric acids were purchased from Sigma (DNO_3 : >99% D, 68% solution in D_2O ; D_2SO_4 : >99.5% D, 98% solution in D_2O).

After passivation of the halocarbon-wax-coated vacuum manifold by repeated exposures to the gas of interest, at least 10 Torr of nitric acid or water vapor was added to the manifold. The gas flowed from there into the Knudsen cell via a stainless steel needle valve, entering the cell through small holes in a ring-shaped wax-coated glass injector. Pressures in the Knudsen cell were monitored by a capacitance pressure manometer (Edwards 570AB, 1 Torr range). Gases exiting the Knudsen cell passed through a differential pumping chamber into the mass spectrometer through a pinhole and tuning fork chopper. Pressures in both chambers were monitored using ionization gauges. Nitric acid was detected using quadrupole mass spectrometry (Extranuclear Laboratories, Inc., EMBA II) by selectively monitoring the ions at $m/z = 64$ (DNO_3^+), 63 (HNO_3^+), 46 (NO_2^+), and 30 (NO^+) using Teknivent Vector/One spectrometer control software. Ion current signals from the mass spectrometer were processed by a lock-in amplifier

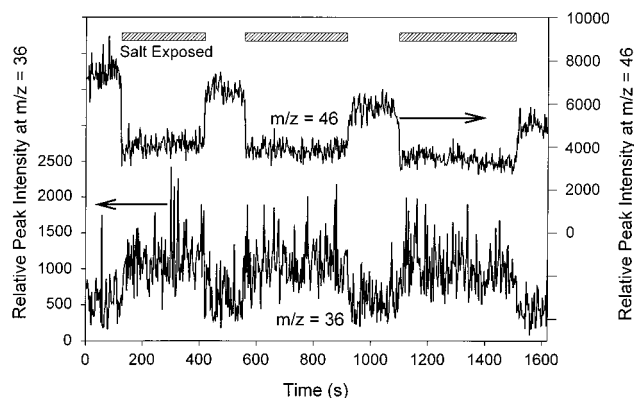


Figure 1. Uptake of HNO_3 on fine synthetic sea salt heated for 25 h prior to reaction and production of HCl . $[\text{HNO}_3]_0 = 2.6 \times 10^{12}$ molecules cm^{-3} . Geometric SSS surface area = 745 mm^2 . Exit aperture diameter is 9 mm. Upper trace (right axis): NO_2^+ mass spectrometer signals ($m/z = 46$). Lower trace (left axis): HCl^+ signals ($m/z = 36$). Hatched bars at top denote when the cover over SSS is open and reaction is occurring. The continuous decline in the HNO_3 signal at $m/z = 46$ is due to a slow decrease in the flow rate of HNO_3 into the cell.

(EG&G Princeton Applied Research Model 5209) at the chopping frequency (800 Hz) and recorded by a PC.

All nitric acid uptake data are based on signals of the most abundant ion (NO_2^+), but NO^+ was monitored in every experiment to ensure that $\text{NO}_2^+/\text{NO}^+$ ratios remained consistent with fragmentation of only HNO_3 parent molecules. The weak molecular HNO_3^+ and DNO_3^+ ions were used to ascertain the purity of DNO_3 vapor by comparison of the correlation of each ion signal to strong NO_2^+ signals as the flow of nitric acid was turned on and off. H_2O^+ , HDO^+ , and D_2O^+ signals were monitored to determine background H/D ratios in the vacuum chamber. Detection limits for HNO_3 (at $m/z = 46$) ranged from 4×10^{10} to $6 \times 10^{11} \text{ cm}^{-3}$. Typical nitric acid concentrations during uptake experiments were in the range $(0.6\text{--}9.7) \times 10^{12}$ molecules cm^{-3} .

Results and Discussion

Reaction of HNO_3 with Synthetic Sea Salt. Figure 1 shows typical NO_2^+ data at $m/z = 46$ for the uptake of HNO_3 by synthetic sea salt which had been heated for 25 h while pumping. The lid covering the sample was opened and closed repetitively. Periods when the lid was open, allowing the gas to react with the surface, are marked with a hatched bar. The uptake of HNO_3 by the salt is clearly seen whenever the lid is opened. The differences between the signals at $m/z = 46$ with the lid opened and closed were used with eq 1 to derive reaction probabilities.

Gas-phase HCl at $m/z = 36$ is the only product, as expected, and is observed above baseline levels only when the salt is exposed to HNO_3 . In several experiments, both HNO_3 ($m/z = 46$, NO_2^+) and HCl ($m/z = 36$) signals were calibrated separately, giving an average product yield of $95 \pm 32\%$ (1σ).

Figure 2 shows the nitric acid reaction probabilities as a function of time for the experiment in Figure 1. The reaction probability declines from an initial value, γ_{init} , by $\sim 50\%$ during the first 1000 s and then remains relatively constant (to within $\sim 20\%$) at a steady-state value, γ_{ss} . While this relative decline in uptake was observed in each experiment, regardless of the pretreatment of the salt, the absolute values of both γ_{init} and γ_{ss} depended on the salt heating time prior to the reaction. This effect is shown in Figure 3 for a collection of HNO_3 and DNO_3 uptake measurements. Initial reaction probabilities (γ_{init}) greater than 0.3 were measured on synthetic sea salt samples that had not been heated. On the other hand, $\gamma_{\text{init}} \approx 0.08$ for salts that

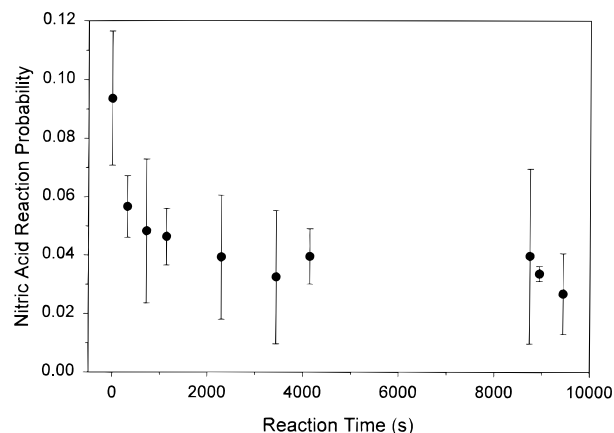


Figure 2. Dependence of nitric acid reaction probabilities on HNO_3 reaction time under same conditions as Figure 1. All data points except the first and last are weighted averages of the measurements made while sequentially opening and closing the lid over the sample.

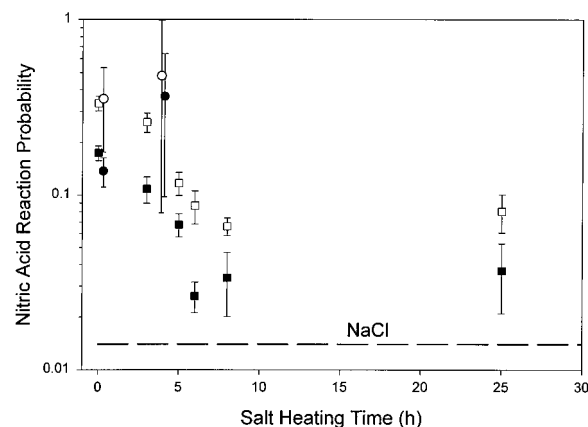


Figure 3. Measured reaction probabilities for nitric acid with synthetic sea salt and $\text{MgCl}_2 \cdot 6\text{H}_2\text{O}$ as a function of heating time immediately prior to HNO_3 exposure. (\square) Initial reaction probabilities for SSS. The two points at zero heating time represent the weighted average of four runs each, with the remainder representing individual runs. (\blacksquare) Steady-state reaction probabilities for SSS. (\circ) Initial reaction probabilities on $\text{MgCl}_2 \cdot 6\text{H}_2\text{O}$. (\bullet) Steady-state reaction probabilities on $\text{MgCl}_2 \cdot 6\text{H}_2\text{O}$. Dashed line: steady-state reaction probabilities on NaCl .⁵⁸ A log scale has been used to show NaCl , SSS, and $\text{MgCl}_2 \cdot 6\text{H}_2\text{O}$ data in the same figure. All error bars are $\pm 2\sigma$.

had been heated for 6 h or more, with heating for shorter times giving reaction probabilities between these two extremes. Steady-state reaction probabilities show the same trend.

Two measurements of nitric acid uptake were also performed on unground samples of magnesium chloride hexahydrate, the most abundant crystalline hydrate in SSS which had been heated for either 0 or 4 h. Reaction probabilities were always greater than 0.1. This suggests that the high reactivity of SSS may be determined, at least in part, by such crystalline hydrates, consistent with earlier studies.⁵⁷

In one run (not shown in Figure 3) a synthetic sea salt sample was heated while pumping for approximately 22 h. Then, in a departure from normal procedures where the salt is covered while still hot, the sample was pumped for 6 h as it cooled prior to exposure to HNO_3 . Nitric acid was taken up at very high rates onto this surface at first exposure ($\gamma_{\text{init}} = 0.75_{-0.68}^{+0.25}$), suggesting that the salt surface reequilibrated with water in the Knudsen cell as it cooled. Although the absolute background pressure in the cell is not routinely measured, a pressure of 10^{-6} Torr would be typical under these conditions. Assuming that this background pressure is laboratory air at 50% relative humidity, the background water vapor pressure is $5 \times$

TABLE 1: Uptake of HNO₃ on Synthetic Sea Salt and MgCl₂·6H₂O at 298 K^a

expt no.	salt wt (g)	no. of layers ^f	salt type	surf. area (mm ²)	[HNO ₃] ₀ (10 ¹² cm ⁻³)	heating time (h)	initial γ ($\pm 2\sigma$) ^b	steady-state γ^i ($\pm 2\sigma$) ^b
1 ^{c,d}	1.13	2.4	SSS-coarse	745	8.1	6 ^g	0.087 \pm 0.019	0.026 \pm 0.005
2 ^d	0.364	7.8 \times 10 ²	SSS-fine	745	6.5	8	0.066 \pm 0.008	0.034 \pm 0.013
3	0.820	1.7 \times 10 ³	SSS-fine	745	2.6	25	0.093 \pm 0.023	0.037 \pm 0.016
4	0.960	2.0	SSS-coarse	745	1.3	0	0.36 ^{+0.64} _{-0.35}	0.25 ^{+0.31} _{-0.23}
5	2.37	2.0	SSS-coarse	1886	0.6	0	0.43 ^{+0.57} _{-0.42}	0.15 ^{+0.24} _{-0.14}
6	2.95	2.5	SSS-coarse	1886	1.6	22 ^h	0.75 ^{+0.25} _{-0.68}	0.13 \pm 0.02
7 ^e	0.843	1.8	SSS-coarse	745	2.3	0	0.67 \pm 0.34	0.23 \pm 0.10
8	1.08	2.3	SSS-coarse	745	2.9	3	0.26 \pm 0.03	0.11 \pm 0.02
9	0.878	1.9 \times 10 ³	SSS-fine	745	9.7	5	0.12 \pm 0.02	0.068 \pm 0.010
10	0.623	1.3 \times 10 ³	SSS-fine	745	8.1	0	0.33 \pm 0.03	0.17 \pm 0.02
11	0.911	1.1	MgCl ₂ ·6H ₂ O-coarse	745	1.6	4	0.48 \pm 0.40	0.37 \pm 0.27
12	1.37	1.7	MgCl ₂ ·6H ₂ O-coarse	745	5.2	0	0.35 \pm 0.18	0.14 \pm 0.03

^a Aperture was 9 mm in diameter except where indicated. ^b Errors are statistical errors only, based on errors in N_0 and N_r . ^c Aperture was 5 mm diameter. ^d Reactant was DNO₃. ^e Salt exposed to D₂O before HNO₃ reaction. ^f Estimate based on mass of salt, density, geometric area of the sample, and a typical SSS particle diameter of 300 μ m for coarse particles and 0.3 μ m for fine particles; typical diameter of coarse MgCl₂·6H₂O was 700 μ m. ^g Heated and pumped for 3 h, stored under UHP He for 2 weeks, and then heated and pumped for 3 h immediately before the experiment. ^h Pumped for 6 h at room temperature after heating. ⁱ Reaction probabilities at 1500 s reaction time.

10⁸ molecules cm⁻³. At this pressure, the time to completely saturate the surface if the uptake coefficient was unity would be several minutes and correspondingly longer with smaller uptake coefficients. While water is not readily taken up on the (100) surface of NaCl at room temperature,^{59,63–67} it is clear from experiments described below that it is much more readily taken up on SSS. Hence, uptake of significant amounts of water on the SSS over 6 h with the sample lid open is not surprising.

Table 1 summarizes the measured reaction probabilities for HNO₃ with SSS and MgCl₂·6H₂O. The data clearly suggest that the major determinant of reaction probabilities is the amount of water available on the salt for uptake of HNO₃, which is affected by the amount of heating and pumping of the salt prior to reaction. For similar salt pretreatments, the value of the reaction probability for SSS did not depend on the geometric salt surface area, particle size, the number of layers of salt particles, or the size of the exit aperture. The smallest particles were prepared by mechanical grinding which may increase the number of surface defects, while the coarse ones were used as received. However, there was no significant difference in the reaction probability for these two types of powders, suggesting that defect sites generated in the grinding process do not play a major role. While there was a slight trend to larger values (by \sim 25%) for the reaction probabilities using the drop in signal on opening the lid compared to those derived from the increase upon closing it, they were within experimental error of each other.

Corrections to the measured reaction probabilities for diffusion into the salt sample are controversial.^{37,38,41,43,58} As was the case in earlier studies of the NaCl reaction,⁵⁸ the reaction probabilities measured here were not sensitive to the number of salt layers. This indicates that diffusion into pores between the salt crystals followed by reaction is not important. In addition, the reaction probabilities of HNO₃ with synthetic sea salt for many experimental conditions are large enough ($\gamma \geq 0.1$) that HNO₃ will be taken up on the first few collisions with the surface. Significant diffusion into the salt is therefore not expected, and corrections for increased surface area due to these pores would be small for such cases. Because of these factors, our measurements are reported without corrections for internal surface area. However, as discussed in more detail below, different regions of the surface may not be equally reactive due to the heterogeneous nature of synthetic sea salt. Hence, the use of the geometric area results in an overall reaction probability and may underestimate the value for the more

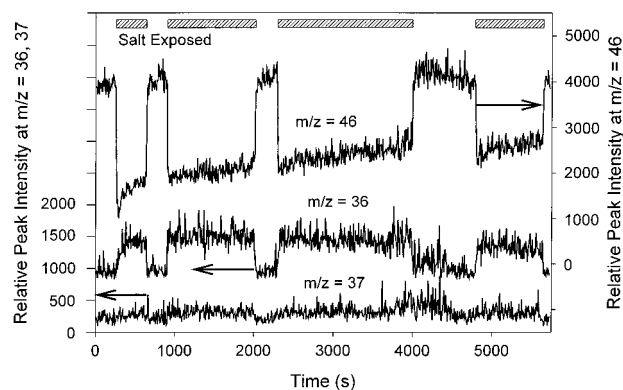


Figure 4. Uptake of DNO₃ on coarse synthetic sea salt, which had been heated for 6 h prior to reaction, and production of HCl and DCl. [DNO₃]₀ = 8.1 \times 10¹² molecules cm⁻³. Geometric SSS surface area = 745 mm². Exit aperture = 5 mm. DNO₃ is monitored using the NO₂⁺ fragment at m/z = 46 and HCl and DCl signals at m/z = 36 and 37, respectively.

reactive components and overestimate that for the less reactive components.

Fenter et al.⁶⁸ used Monte Carlo simulations to examine potential systematic errors in Knudsen cell experiments. The effects of surface-to-volume ratio, position of injection of the reactant gas, reactor geometry, and reactive surface area were all examined. For very fast uptake, approaching unity, diffusion effects may potentially introduce systematic error, depending on the injector position relative to the reactive surface. However, for the largest reaction probabilities reported in our experiments, the error bars based on statistical errors in N_0 and N_r were large, encompassing unity (Table 1). As a result, no attempt was made to correct these larger reaction probabilities for such smaller, potential systematic errors.

Role of Water in Uptake of Nitric Acid. Given the critical role of surface water in the uptake of HNO₃ on pure NaCl,⁵⁸ it is not surprising that water also controls the reaction on SSS, which contains highly hygroscopic salts such as MgCl₂·6H₂O. Two types of experiments were carried out to probe for surface water on SSS: a search for the production of HCl from the reaction of DNO₃ and measurements of the uptake of D₂O with production of HDO and H₂O.

Reaction of DNO₃. The uptake of DNO₃ onto synthetic sea salt and the production of HCl is shown in Figure 4. A sharp drop in the signal at m/z = 46 as the salt surface is exposed

indicates DNO_3 uptake, which begins with $\gamma_{\text{init}} = 0.087 \pm 0.019$ at first exposure and decreases to $\gamma_{\text{ss}} = 0.026 \pm 0.005$. HCl ($m/z = 36$) is produced, but DCl signals (at $m/z = 37$) are too small to be readily discernible in Figure 4. In the absence of a strongly adsorbed H_2O layer, only the production of DCl should be observed from this reaction of DNO_3 with SSS.

Isotope exchange between DCl and HCl can occur readily in vacuum systems, potentially contributing to the observation of HCl during the reaction of DNO_3 . To test for this possibility, two sets of measurements were performed. First, the isotopic purity of DNO_3 was measured in several runs by monitoring the weak parent HNO_3 and DNO_3 ions immediately before the experiment. The dominant source of HNO_3 impurity in DNO_3 is the interaction of DNO_3 with the walls of the vacuum line before entry into the Knudsen cell. Conditioning the walls by sequential exposures to a few Torr of DNO_3 increased the measured isotopic DNO_3 purity to a typical value of $90 \pm 32\%$. The corresponding ratio of product HCl/DCl from the reaction of DNO_3 with SSS in these runs was 3.8 ± 1.1 (weighted average), well in excess of the maximum HNO_3 impurity in the DNO_3 source.

The ratio of hydrogen to deuterium atoms due to background levels of H_2O , HDO , and D_2O in the mass spectrometer was also measured. The H/D ratio is a measure of the expected HCl/DCl ratio if the appearance of HCl was due solely to proton exchange of DCl product with water at the Knudsen cell and vacuum chamber walls. During experiments using DNO_3 , the H/D ratio measured using background signals at $m/z = 18, 19$, and 20 was typically 1.8 ± 0.9 , again significantly lower than the HCl/DCl ratio of 3.8 ± 1.1 from the reaction of DNO_3 with SSS.

In short, water available at the surface of synthetic sea salt must be the major source of hydrogen atoms in the measured HCl product.

Uptake of D_2O and Formation of HDO and H_2O . In previous experiments, the uptake of water on ground NaCl powders was not observable, even in pulsed experiments,³⁷ and upper limits of $\gamma < 2 \times 10^{-4}$ and $\sim 10^{-5}$ were reported.^{37,58} However, isotopic studies of nitric acid uptake suggested that adsorbed water was nevertheless present on the surface.⁵⁸ The adsorbed water was hypothesized to be in a fast equilibrium with the gaseous H_2O added to the Knudsen cell, so that there was no net uptake. Since SSS should hold much larger quantities of surface water, this hypothesis was examined by studying the uptake of D_2O and the displacement of adsorbed H_2O and HDO on synthetic sea salt powders, as well as on NaCl for comparison.

The loss of D_2O and the production of HDO and H_2O would be very brief if the amount of surface adsorbed water is small compared to the amount of D_2O which can be taken up from the gas phase. Water uptake on NaCl surfaces was therefore first studied using low D_2O concentrations near the detection limit. No significant uptake was observed, from which an upper limit to the uptake probability of $\gamma_{\text{D}_2\text{O}} \leq 0.02$ was derived, consistent with earlier studies.⁵⁸

However, large D_2O uptake rates were observed on synthetic sea salt surfaces. Typical data are shown in Figure 5 for 0.84 g of coarse SSS crystals which had not been heated prior to reaction. HDO ($m/z = 19$) is produced in large quantities, along with smaller amounts of H_2O ($m/z = 18$). D_2O signals (at $m/z = 20$) drop rapidly at the first exposure. Initial D_2O uptake probabilities were greater than 0.3 on all fresh synthetic sea salt surfaces and were in the range $0.05 < \gamma < 0.25$ for SSS surfaces that had previously been exposed to nitric acid. Uptake probabilities decreased with reaction time, as expected if the

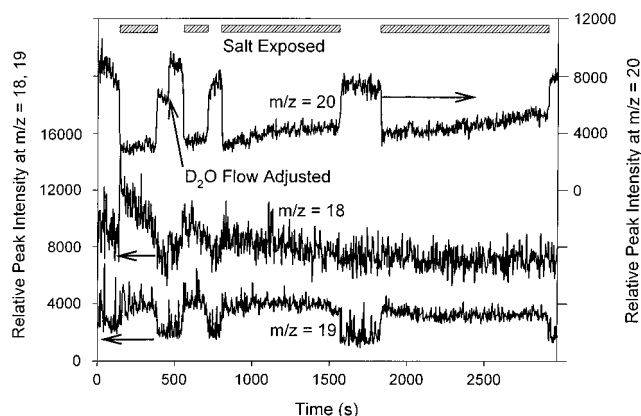


Figure 5. Uptake of D_2O on 0.84 g of coarse synthetic sea salt surfaces not heated prior to reaction. $[\text{D}_2\text{O}]_0 = 6.5 \times 10^{12} \text{ molecules cm}^{-3}$. Geometric SSS surface area = 745 mm^2 . Exit aperture diameter was 9 mm. Upper trace: mass spectrometric D_2O^+ signals at $m/z = 20$ (right axis). Middle trace: H_2O^+ signal at $m/z = 18$ (left axis, shifted up by 3000 counts for clarity); approximately 5% of the signal at $m/z = 18$ is due to OD^+ fragments from HDO and D_2O , rather than H_2O^+ . Lower trace: signal at $m/z = 19$ for HDO^+ (left axis).

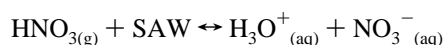
surface water is being slowly converted from H_2O to D_2O . For example, in another experiment using 1.29 g of SSS which had been heated for 5 h, D_2O uptake probabilities declined from an initial value of $0.9^{+0.1}_{-0.8}$ to 7×10^{-3} over the course of about 3 h. This is expected once replacement of the original surface H_2O by D_2O is complete, since simultaneous uptake and evaporation of D_2O do not lead to a net, measurable, uptake of D_2O .

An estimate of the original amount of water on the surface that can be replaced by D_2O was obtained for the experiment in which D_2O exposure was continued for 3 h. The signals from HDO and H_2O decay with time as D_2O is taken up and the original surface H_2O is replaced by D_2O . These signals at $m/z = 19$ and 18 (corrected for the contribution of OD^+ fragments), which are proportional to the total number of HDO and H_2O formed, were integrated as a function of time. The integrated areas were converted to absolute numbers of HDO and H_2O by comparison to the integrated signals from the decay of a known initial concentration of D_2O in the cell. Given the small differences in molecular weight between D_2O , HDO , and H_2O , this decay, as well as the mass spectrometer sensitivity to each compound, was assumed to be the same for all three. The total numbers of HDO and H_2O released from this salt sample were thus calculated to be $(2.8 \pm 1.0) \times 10^{18}$ and $(1.8 \pm 0.6) \times 10^{17}$ molecules, respectively, which corresponds in total H atoms to the displacement of $(1.6 \pm 0.5) \times 10^{18}$ H_2O molecules. The estimated amount of water originally on the surface that is available for replacement by D_2O is thus $(1.6 \pm 0.5) \times 10^{18}$ H_2O molecules for 1.29 g of SSS with a geometric surface area of 745 mm^2 which had been heated for 5 h.

An estimate of the net growth of the adsorbed water layer can also be obtained by integrating the total uptake of D_2O over the course of the experiment, which in this case was $(6.0 \pm 2.0) \times 10^{18}$ molecules. Since a total of $(3.0 \pm 1.0) \times 10^{18}$ molecules of combined $\text{HDO} + \text{H}_2\text{O}$ were displaced as the D_2O was taken up, there was a net addition of $(3.0 \pm 2.2) \times 10^{18}$ water molecules to the synthetic sea salt surface. Since the original amount of water available was $(1.6 \pm 0.5) \times 10^{18}$ molecules, the amount of water available on the surface has nearly tripled.

In short, there are clearly substantial amounts of water on the surface of synthetic sea salt, even after gentle heating and pumping, and the salt can take up significant additional amounts.

The model⁵⁸ developed for reaction of HNO₃ with NaCl powders is rapid uptake of HNO₃ from the gas phase into the surface-adsorbed water (SAW) which leads to acidification of the SAW:



The SAW is assumed to be initially saturated in Na⁺ and Cl⁻. When the SAW becomes sufficiently acidic, HCl degasses. As HNO₃ continues to be taken up into the SAW, nitrate can be removed by precipitation onto the salt surface as NaNO₃. This model explains why the surface does not become "saturated", since nitrate and HCl are continuously removed, allowing further uptake of HNO₃.

The current results on reaction of HNO₃ with SSS are consistent with this model. First, the trend to lower reaction probabilities with increased salt heating prior to reaction (Figure 3) suggests that SAW is again controlling the uptake and reaction of HNO₃. Second, exposure of SSS to 0.2 mTorr of H₂O for 50 min, followed by 2 mTorr of H₂O for 4 min immediately prior to a nitric acid uptake experiment, gave one of the highest steady-state reaction probabilities observed in this study, $\gamma_{\text{ss}} = 0.23 \pm 0.10$. This high reaction probability can be attributed to enlarged SAW, since the D₂O experiments described earlier indicated a net uptake of water onto hygroscopic SSS surfaces, even at these low water vapor pressures. Third, the reaction probabilities for SSS even with extensive preheating are always at least a factor of 2 greater than for NaCl, where the amount of SAW is sufficiently small that it could not be readily estimated.

As discussed above, significant D₂O uptake and the production of HDO and H₂O are observed for SSS, which led to an estimate of 1.6×10^{18} H₂O molecules initially on the surface. This corresponds to a volume of ~50 nL. According to the model proposed for NaCl,⁵⁸ if the SAW is saturated in NaCl, HNO₃ will be taken up in larger quantities initially until the SAW reaches equilibrium at a pH of ~1.7. At this point, continued uptake of HNO₃ and degassing of HCl occurs in a steady-state fashion. For a SAW volume of 50 nL assumed to be spread equally over the geometric surface area (which is unlikely; see below) and an initial uptake coefficient for HNO₃ of 0.1, the time to acidify the SAW to this pH is in the range of approximately 20–120 ms for the HNO₃ concentrations used here. Hence, while there should be a larger initial uptake of HNO₃ and an induction period for the generation of HCl, these occur on a time scale too short to be measured with the current apparatus.

The surface water is highly unlikely to be distributed evenly over all of the component salt crystals. NaCl is a major component of sea salt. The NaCl (100) surface is known not to take up significant amounts of water at the low water vapor pressures in our vacuum system.^{59,63–67} However, recent atomic force microscopy studies suggest that there may be voids in the NaCl crystal surface which hold 3D water,⁶² and these may be the sites for SAW observed in the previous studies of the NaCl reaction with HNO₃.⁵⁸ However, with synthetic sea salt there are also highly hygroscopic components such as MgCl₂·6H₂O whose deliquescence point is 33% at 298 K based on the activity of water in the bulk saturated solution.⁶⁹ The contribution of hygroscopic salts is supported by the large reaction probabilities measured in the two experiments with MgCl₂·6H₂O. The presence of such salts would be expected to give a larger effective SAW area for uptake of HNO₃ compared to pure NaCl, leading to a larger steady-state reaction probability. This is indeed what is observed, where γ_{ss} for unheated synthetic sea salt is approximately an order of magnitude larger than for NaCl.

In addition to water adsorbed on the surface, there is also water available in the crystal lattice of the hydrates such as MgCl₂·6H₂O. This water is bound in the crystal lattice⁷⁰ and is not expected to behave as a quasi-liquid layer. Gentle heating of these hydrates at 75–80 °C does not lead to significant dehydration of the MgCl₂·6H₂O,⁷¹ so that the major effect of heating must be to remove some of the physisorbed water. However, the results of earlier infrared studies⁵⁷ of the reaction of SSS with NO₂ and HNO₃ suggested that reaction of these hydrates disrupted the crystal lattice, releasing some of the waters of hydration originally bound in the crystal lattice. How much such a process contributes to the surface water in the present case is not known.

Atmospheric Implications. The results of these studies show that the reaction probability of nitric acid with atmospheric sea salt aerosol is larger than assumed using the NaCl reaction as a surrogate for sea salt particles. The synthetic sea salt surfaces that were not heated immediately prior to exposure to HNO₃ are most representative of real sea salt aerosol at low relative humidities where the particles have not deliquesced. A reaction probability of $\gamma \sim 0.2$ is suggested based on steady-state HNO₃ uptake rates.

This reaction probability is greater than recommendations based on NaCl studies^{37,38,41,58} by approximately an order of magnitude, suggesting an increased importance of the HNO₃ reaction relative to those generating photochemically active halogen compounds. However, Behnke and Zetzsch^{29,33} have reported that other reactions generating atomic chlorine are also accelerated on sea salt relative to NaCl aerosol. It is clear that in order to quantify the production of atomic chlorine and HCl in the marine boundary layer and in coastal areas, measurements of the heterogeneous reactions of other relevant gases with sea salt surfaces are needed. Studies of the reactions of N₂O₅ and ClONO₂ are currently underway in this laboratory.

Conclusions

Nitric acid uptake on synthetic sea salt is fast. Reaction probabilities are shown to depend on salt heating times immediately prior to reaction, which drives water off the surface. Uptake studies of DNO₃ and D₂O demonstrated the presence of extensive surface water on SSS surfaces, even samples that were heated while pumping for extensive periods. This is likely due in large part to the presence of hygroscopic crystalline hydrates such as MgCl₂·6H₂O. These studies confirm the key role of surface-adsorbed water on the uptake and reaction of HNO₃ with sea salt and its components. Under atmospheric conditions, the estimated reaction probability for HNO₃ with synthetic sea salt is ~0.2, at least an order of magnitude faster than for reaction with NaCl.

Acknowledgment. The authors thank the National Science Foundation (Grant No. ATM-9302475), the Department of Energy (Grant No. DE-FG 03-94ER61899), and the Joan Irvine Smith and Athalie R. Clarke Foundation for support of this work. We are also grateful to F. J. Feher for helpful discussions and to G. E. Ewing and M. J. Rossi for providing preprints prior to publication.

References and Notes

- (1) Solomon, S.; Borrmann, S.; Garcia, R. R.; Portmann, R.; Thomason, L.; Poole, L. R.; Winker, D.; McCormick, M. P. *J. Geophys. Res.* **1997**, *102*, 21411.
- (2) Finlayson-Pitts, B. J.; Pitts, J. N., Jr. *Atmospheric Chemistry: Fundamentals and Experimental Techniques*; Wiley-Interscience: New York, 1986.
- (3) Finlayson-Pitts, B. J. *Res. Chem. Intermed.* **1993**, *19*, 235.

- (4) Graedel, T. E.; Keene, W. C. *Global Biogeochem. Cycles* **1995**, *9*, 47.
- (5) Keene, W. C. Inorganic Cl Cycling in the Marine Boundary Layer: A Review. *Naturally-Produced Organohalogenes*; Grimvall, A., de Leer, E. W. B., Eds.; Kluwer Academic Publishers: Dordrecht, The Netherlands, 1995; pp 363–373.
- (6) Andreae, M. O.; Crutzen, P. J. *Science* **1997**, *276*, 1052.
- (7) Finlayson-Pitts, B. J.; Pitts, J. N., Jr. *Science* **1997**, *276*, 1045.
- (8) Ravishankara, A. R. *Science* **1997**, *276*, 1058.
- (9) O'Dowd, C. D.; Smith, M. H.; Consterdine, I. E.; Lowe, J. A. *Atmos. Environ.* **1997**, *31*, 73.
- (10) Tang, I. N.; Munkelwitz, H. R.; Davis, J. G. *J. Aerosol. Sci.* **1977**, *8*, 149.
- (11) Moyers, J. L.; Duce, R. A. *J. Geophys. Res.* **1972**, *77*, 5330.
- (12) Cicerone, R. J. *Rev. Geophys. Space Phys.* **1981**, *19*, 123.
- (13) Keene, W. C.; Pszenny, A. A. P.; Jacob, D. J.; Duce, R. A.; Galloway, J. N.; Schultz-Tokos, J. J.; Sievering, H.; Boatman, J. F. *Global Biogeochem. Cycles* **1990**, *4*, 407.
- (14) Robbins, R. C.; Cadle, R. D.; Eckhardt, D. L. *J. Met.* **1959**, *16*, 53.
- (15) Cadle, R. D.; Robbins, R. C. *Discuss. Faraday Soc.* **1960**, *30*, 155.
- (16) Schroeder, W. H.; Urone, P. *Environ. Sci. Technol.* **1974**, *8*, 756.
- (17) Chung, T. T.; Dash, J.; O'Brien, R. J. *9th Int. Congr. Electron Microsc.* **1978**, 440.
- (18) Sverdrup, G. M.; Kuhlman, M. R. Heterogeneous Nitrogen Oxide-Particle Reactions. *Atmospheric Pollution, Proceedings of the 14th International Colloquium, Paris, France, May 5–8, 1980*; Benarie, M. M., Ed.; Elsevier Scientific: Amsterdam, 1980.
- (19) Finlayson-Pitts, B. J. *Nature* **1983**, *306*, 676.
- (20) Zetzsch, C. Simulation of Atmospheric Photochemistry in the Presence of Solid Airborne Aerosols. In *Formation, Distribution and Chemical Transformation of Air Pollutants*; Zellner, R., Ed.; Monograph 104; VCH Publishers: Frankfurt, 1987; pp 187–212.
- (21) George, Ch.; Ponche, J. L.; Mirabel, Ph.; Behnke, W.; Scheer, V.; Zetzsch, C. *J. Phys. Chem.* **1994**, *98*, 8780.
- (22) Zetzsch, C.; Behnke, W. *Ber. Bunsen-Ges. Phys. Chem.* **1992**, *96*, 488.
- (23) Zetzsch, C.; Behnke, W. Heterogeneous Reactions of Chlorine Compounds. In *The Tropospheric Chemistry of Ozone in the Polar Regions*; Niki, H., Becker, K. H., Eds.; Springer-Verlag: Berlin, 1993; pp 291–306.
- (24) Finlayson-Pitts, B. J.; Ezell, M. J.; Pitts, J. N., Jr. *Nature* **1989**, *337*, 241.
- (25) Finlayson-Pitts, B. J.; Livingston, F. E.; Berko, H. N. *J. Phys. Chem.* **1989**, *93*, 4397.
- (26) Finlayson-Pitts, B. J.; Livingston, F. E.; Berko, H. N. *Nature* **1990**, *343*, 622.
- (27) Behnke, W.; Zetzsch, C. *J. Aerosol Sci.* **1989**, *20*, 1167.
- (28) Behnke, W.; George, C.; Scheer, V.; Zetzsch, C. *J. Geophys. Res.* **1997**, *102*, 3795.
- (29) Behnke, W.; Zetzsch, C. *J. Aerosol Sci.* **1990**, *21*, S229.
- (30) Mamane, Y.; Gottlieb, J. *J. Aerosol Sci.* **1990**, *21*, S225.
- (31) Behnke, W.; Kruger, H.-U.; Scheer, V.; Zetzsch, C. *J. Aerosol Sci.* **1991**, *22*, S609.
- (32) Behnke, W.; Scheer, V.; Zetzsch, C. *J. Aerosol Sci.* **1994**, *25*, S277.
- (33) Behnke, W.; Scheer, V.; Zetzsch, C. Production of a Photolytic Precursor of Atomic Cl from Aerosols and Cl⁻ in the Presence of O₃. In *Naturally-Produced Organohalogenes*; Grimvall, A., de Leer, E. W. B., Eds.; Kluwer Academic Publishers: Dordrecht, The Netherlands, 1995; pp 375–384.
- (34) Livingston, F. E.; Finlayson-Pitts, B. J. *Geophys. Res. Lett.* **1991**, *18*, 17.
- (35) Winkler, T.; Goschnick, J.; Ache, H. J. *J. Aerosol Sci.* **1991**, *22*, S605.
- (36) Junkermann, W.; Ibusuki, T. *Atmos. Environ.* **1992**, *26A* 3099.
- (37) Fenter, F. F.; Caloz, F.; Rossi, M. J. *J. Phys. Chem.* **1994**, *98*, 9801.
- (38) Fenter, F. F.; Caloz, F.; Rossi, M. J. *J. Phys. Chem.* **1996**, *100*, 1008.
- (39) Timonen, R. S.; Chu, L. T.; Leu, M.-T.; Keyser, L. F. *J. Phys. Chem.* **1994**, *98*, 9509.
- (40) Peters, S. J.; Ewing, G. E. *J. Phys. Chem.* **1996**, *100*, 14093.
- (41) Leu, M.-T.; Timonen, R. S.; Keyser, L. F.; Yung, Y. L. *J. Phys. Chem.* **1995**, *99*, 13203.
- (42) Karlsson, R.; Ljungström, E. *J. Aerosol Sci.* **1995**, *26*, 39.
- (43) Leu, M.-T.; Timonen, R. S.; Keyser, L. F. *J. Phys. Chem. A* **1997**, *101*, 278.
- (44) Caloz, F.; Fenter, F. F.; Rossi, M. J. *J. Phys. Chem.* **1996**, *100*, 7494.
- (45) DeMore, W. B.; Sander, S. P.; Golden, D. M.; Hampson, R. F.; Kurylo, M. J.; Howard, C. J.; Ravishankara, A. R.; Kolb, C. E.; Molina, M. J. *Chemical Kinetics and Photochemical Data for Use in Stratospheric Modeling*, Evaluation No. 12, JPL Publ. No. 97-4, January 15, 1997.
- (46) Singh, H. B.; Kastig, J. F. *J. Atmos. Chem.* **1988**, *7*, 261.
- (47) Keene, W. C.; Jacob D. J.; Fan, S.-M. *Atmos. Environ.* **1996**, *30* i.
- (48) Spicer, C. W.; Chapman, E. G.; Finlayson-Pitts, B. J.; Plastringe, R. A.; Hubbe, J. M.; Fast, J. D.; Berkowitz, C. M. Manuscript in preparation.
- (49) Pszenny, A. A. P.; Keene, W. C.; Jacob, D. J.; Fan, S.; Maben, J. R.; Zetwo, M. P.; Springer-Young, M.; Galloway, J. N. *Geophys. Res. Lett.* **1993**, *20*, 699.
- (50) Impey, G. A.; Shepson, P. B.; Hastie, D. R.; Barrie, L. A.; Anlauf, K. *J. Geophys. Res.* **1997**, *102*, 16005.
- (51) Jobson, B. T.; Niki, H.; Yokouchi, Y.; Bottenheim, J.; Hopper, F.; Leaitch, R. *J. Geophys. Res.* **1994**, *99*, 25355.
- (52) Wingenter, O. W.; Kubo, M. K.; Blake, N. J.; Smith, T. W., Jr.; Blake, D. R.; Rowland, F. S. *J. Geophys. Res.* **1996**, *101*, 4331.
- (53) Singh, H. B.; Gregory, G. L.; Anderson, B.; Browell, E.; Sachse, G. W.; Davis, D. D.; Crawford, J.; Bradshaw, J. D.; Talbot, R.; Blake, D. R.; Thornton, D.; Newell, R.; Merrill, J. *J. Geophys. Res.* **1996**, *101*, 1907.
- (54) Singh, H. B.; Thakur, A. N.; Chen, Y. E.; Kanakidou, M. *Geophys. Res. Lett.* **1996**, *23*, 1529.
- (55) Rudolph, J.; Koppmann, R.; Plass-Dulmer, Ch. *Atmos. Environ.* **1996**, *30*, 1887.
- (56) Kester, D. R.; Duedall, I. W.; Connors, D. N.; Pytkowicz, R. M. *Limnol. Oceanogr.* **1967**, *12*, 176.
- (57) Langer, S.; Pemberton, R. S.; Finlayson-Pitts, B. J. *J. Phys. Chem. A* **1997**, *101*, 1277.
- (58) Beichert, P.; Finlayson-Pitts, B. J. *J. Phys. Chem.* **1996**, *100*, 15218.
- (59) Dai, D. J.; Peters, S. J.; Ewing, G. E. *J. Phys. Chem.* **1995**, *99*, 10299.
- (60) Laux, J. M.; Fister, T. F.; Finlayson-Pitts, B. J.; Hemminger, J. C. *J. Phys. Chem.* **1996**, *100*, 19891.
- (61) Laux, J. M.; Hemminger, J. C.; Finlayson-Pitts, B. J. *Geophys. Res. Lett.* **1994**, *21*, 1623.
- (62) Shindo, H.; Ohashi, M.; Tateishi, O.; Seo, A. *J. Chem. Soc., Faraday Trans.* **1997**, *93*, 1169.
- (63) Estel, J.; Hoinkes, H.; Kaarmann, H.; Nahr, H.; Wilsch, H. *Surf. Sci.* **1976**, *54*, 393.
- (64) Barraclough, P. B.; Hall, P. G. *Surf. Sci.* **1974**, *46*, 393.
- (65) Fölsch, S.; Henzler, M. *Surf. Sci.* **1991**, *247*, 269.
- (66) Peters, S. J.; Ewing, G. E. *Langmuir*, in press.
- (67) Ewing, G. E.; Peters, S. J. *Surf. Rev. Lett.*, in press.
- (68) Fenter, F. F.; Caloz, F.; Rossi, M. J. *Rev. Sci. Instrum.* **1997**, *68*, 3172.
- (69) Robinson, R. A.; Stokes, R. H. *Electrolyte Solutions*; Butterworth: London, 1970.
- (70) Megaw, H. D. *Crystal Structures*; W. B. Saunders, reprinted by TechBooks, Fairfax, VA, 1973.
- (71) *Gmelins Handbuch der Anorganischen Chemie*; Verlag Chemie: Berlin, 1939; Vol. 27, pp 532–535.